

Topological quantum thermometry

Anubhav Kumar Srivastava,^{1,*} Utso Bhattacharya,¹ Maciej Lewenstein,^{1,2} and Marcin Płodzień^{1,†}

¹*ICFO - Institut de Ciències Fotòniques, The Barcelona Institute of Science and Technology, 08860 Castelldefels (Barcelona), Spain*

²*ICREA, Pg. Lluís Companys 23, 08010 Barcelona, Spain*

An optimal local quantum thermometer is a quantum many-body system that saturates the fundamental lower bound for the thermal state temperature estimation accuracy [L. Correa, et. al., Phys. Rev. Lett. 114, 220405 (2015)]. Such a thermometer has a particular energy level structure with a single ground state and highly degenerated excited states manifold, with an energy gap proportional to the estimated temperature. In this work, we show that the optimal local quantum thermometer can be realized in an experimentally feasible system of spinless fermions confined in a one-dimensional optical lattice described by the Rice-Mele model. We characterize the system's sensitivity to temperature changes in terms of quantum Fisher information and the classical Fisher information obtained from experimentally available site occupation measurements.

Introduction—Quantum thermodynamics provides the necessary framework allowing building quantum thermal devices like quantum heat engines [1–5] or quantum batteries [6–18]. Since most of these devices work in ultra-low temperature regimes of the order of nano- and pico-Kelvin [19–21], there is a constant requirement for higher accuracy of the temperature estimation of such quantum systems [22, 23]. The temperature of a given quantum system is not a quantum mechanical observable but rather a parameter of its quantum state [24, 25], and as a result, temperature estimation corresponds to the quantum estimation problem. The accuracy of any estimation is limited by the quantum Cramér-Rao bound [26, 27] relating maximal sensitivity to the parameter changes given by quantum Fisher information, with the estimated parameter [28–34]. The two main paradigms in quantum thermometry are based on the prior knowledge about the system's temperature. In the global quantum thermometry, there is no prior knowledge about the estimated temperature [35–38]. On the other hand, in the local quantum thermometry, it is assumed that the estimator for the temperature is given, whereas the aim is to minimize the uncertainty of the temperature estimator [39–44].

The optimal local quantum thermometer, saturating the fundamental bound of the system's sensitivity to temperature changes, is a two-level many-body system with a single ground state and degenerated manifold of the excited state, with the energy gap proportional to the estimated temperature [39]. Current theoretical efforts in local quantum thermometry are focused on finding the optimal quantum setups that maximize the sensitivity of the system's thermal state to any temperature changes. Over the recent years, different systems have been proposed as optimal quantum thermometers, including two-component fermions in a one-dimensional harmonic trap [45, 46], thermoelectric systems [47, 48], quantum critical

systems [49–53], quantum dots [54–57], color centers in diamonds [58], single qubit dephasing [59], impurities in Bose-Einstein condensates [60–64] or Fermi gases [65–69], as well as exotic models utilizing Unruh-DeWitt detectors [70], utilizing the Berry phase [71], and recently proposed machine learning techniques in various setups such as spin systems [72–74], impurities in Bose gases [75], and even critical systems [76]. However, to the best of our knowledge, there is no experimentally feasible proposition for a quantum system realizing the energy level structure required by the optimal local quantum thermometer.

In this work, we show that an idealized optimal local quantum thermometer with N -fold degeneracy of the excited state, operating in the sub-nK regime, can be realized in the experimentally feasible system of N spinless fermions in a one-dimensional optical lattice with $L = 2(N + 1)$ sites described by the Rice-Mele Hamiltonian [77], operating in the topological regime. The proposed quantum thermometer can be tuned to the optimal temperature by varying the lattice dimerization and the staggered onsite potential. We characterize the sensitivity of the considered quantum thermometer to the temperature changes in terms of the quantum Fisher information (QFI) and the classical Fisher information (CFI) obtained from the experimentally feasible site occupation measurements.

The Rice-Mele model in the limit of vanishing staggered potential reduces to the Su-Schrieffer-Heeger (SSH) model [78, 79] being one of the simplest condensed matter systems that exhibit topological characteristics (for an extensive review, see [80–83]). The Rice-Mele and SSH models have been experimentally realized in many quantum simulator platforms [84], such as quantum gases in optical lattices [85–91], acoustic systems [92], graphene [93], photonic crystals [94], time crystals [95], and in Rydberg arrays [96–98].

Preliminaries—Let us consider a quantum system described by a Hamiltonian \hat{H}_A in a thermal Gibbs state $\hat{\rho}_{T_A}^A$ at an unknown temperature T_A , and a quantum thermometer described by a Hamiltonian \hat{H}_B in a Gibbs state

* anubhav.srivastava@icfo.eu

† marcin.plodzien@icfo.eu

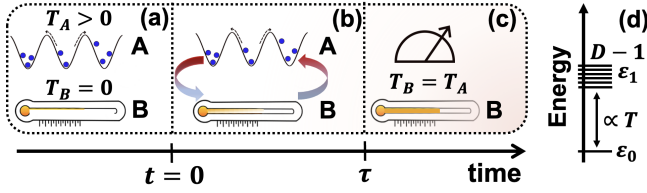


FIG. 1. Schematic representation of a standard thermometry protocol. (a) The quantum thermometer is initially prepared in the pure ground state, (b) and exchanges energy with the system in the Gibbs thermal state at temperature T_A , eventually reaching a thermal state, and lastly, (c) the measurement protocol is prepared to estimate the system's temperature. Panel (d) presents schematically the energy level structure of an optimal quantum thermometer with a single ground state and $(D - 1)$ -fold degeneracy of the excited state [39].

$\hat{\rho}_{T_B}^B$. The quantum thermometer is coupled to system A to exchange energy. After a sufficiently long time, in an ideal scenario, when the larger system acts as a bath, the composite system reaches thermal equilibrium and is described by stationary density matrix $\hat{\rho}^{AB}$. The reduced density matrix of the thermometer $\hat{\rho}_T^B = \text{Tr}_A[\hat{\rho}^{AB}]$ is a thermal state at temperature $T = T_A$, $\hat{\rho}_T^B \simeq \hat{\rho}_T^B$. The measurement protocol is now prepared to estimate the temperature T , now encoded in the thermal state of the thermometer, with high precision as shown in Fig. 1.

The full measurement protocol consists of global thermometry, i.e., estimation of T without prior knowledge about temperature, and local thermometry, which minimizes the standard deviation ΔT of the estimated temperature [39, 42], which is however lower bounded by the quantum Cramér-Rao bound [27, 29] $\Delta T \geq 1/\sqrt{\mathcal{N}\mathcal{F}_T}$, where \mathcal{N} is the prepared number of measurements and \mathcal{F}_T is the quantum Fisher information [26, 28, 30].

The optimal local quantum thermometry aims to find a quantum system maximizing the quantum Fisher information of a thermal state with respect to changes in temperature. The quantum Fisher information for a thermal state $\hat{\rho}_T^B$ reads [26, 99]

$$\mathcal{F}_T = 4 \sum_{l,j} p_l \frac{|\langle \epsilon_l | \partial_T \hat{\rho}_T^B | \epsilon_j \rangle|^2}{(p_l + p_j)^2} = \frac{\Delta \hat{H}_B^2}{T^4}, \quad (1)$$

where $\Delta \hat{H}_B^2 \equiv \text{Tr}[\hat{\rho}_T^B \hat{H}_B^2] - \text{Tr}[\hat{\rho}_T^B \hat{H}_B]^2$, and $\{\epsilon_l, |\epsilon_l\rangle\}_{l=1}^D$ are eigenvalues and eigenvectors of \hat{H}_B , and $\hat{\rho}_T^B = e^{-\beta \hat{H}_B} / \mathcal{Z}$, where $\mathcal{Z} = \sum_l e^{-\beta \epsilon_l}$ and $\beta = 1/k_B T$ (from here on, we introduce the natural constants $k_B = \hbar = 1$), and $p_l = \langle \epsilon_l | \hat{\rho}_T^B | \epsilon_l \rangle = \mathcal{Z}^{-1} e^{-\beta \epsilon_l}$.

As shown in Ref. [39], the variance $\Delta \hat{H}_B^2$ for a thermal state is maximized for the D -dimensional Hamiltonian \hat{H}_B with a two-level energy spectrum having a single ground state, and $(D - 1)$ -fold degenerated excited state, with an energy gap proportional to estimated temperature, i.e. $\epsilon_1 - \epsilon_0 = xT$, where $x > 0$ is the solution of the equation $e^x = (D - 1)(2 + x)/(2 - x)$, see Fig. 1(d).

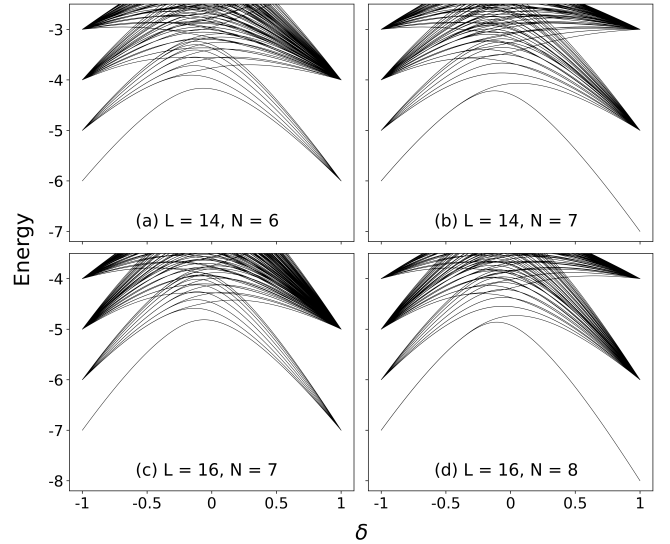


FIG. 2. The energy level structure of the quantum thermometer, Eq. (3) in the SSH limit, i.e. $m = 0$, as a function of the dimerization parameter δ with $N = L/2 - 1$ particles (panels (a)-(c)) and with $N = L/2$ particles (panels (b)-(d)), for system sizes $L = 14$ (panels (a)-(b)) and $L = 16$ (panels (c)-(d)). The optimal local quantum thermometer energy level structure is realized at dimerization limit $\delta = -1$ (topological) with $2N$ -fold degeneracy in the first excited state manifold (panels (a)-(c)), and at $\delta = 1$ (trivial) with N^2 -fold degeneracy (panels (b)-(d)).

In such a case, the QFI for an optimal local quantum thermometer reads [100]

$$\overline{\mathcal{F}}_T = e^x x^2 \frac{D - 1}{(D - 1 + e^x)^2} \frac{1}{T^2}. \quad (2)$$

The model— As a local quantum thermometer, we consider a system of N spinless fermions in a one-dimensional lattice with L sites described by the Rice-Mele Hamiltonian

$$\hat{H}_B = \sum_i (1 + (-1)^i \delta) (\hat{c}_{i+1}^\dagger \hat{c}_i + h.c.) + m \sum_i (-1)^i \hat{n}_i, \quad (3)$$

where \hat{c}_i^\dagger (\hat{c}_i) are the fermionic creation (annihilation) operators acting on the i -th lattice site fulfilling the anti-commutation relation $\{\hat{c}_i, \hat{c}_i^\dagger\} = 1$, $\hat{n}_i = \hat{c}_i^\dagger \hat{c}_i$ is the site occupation operator, $\delta \in [-1, 1]$ is the dimerization parameter, and $m \geq 0$ is the staggered on-site potential strength. The Hilbert space dimension is given by the binomial coefficient $D = \binom{L}{N}$. In the periodic boundary condition geometry, assuming the lattice constant of unit length, the single particle Hamiltonian, Eq. (3), can be expressed in the momentum representation as a two-band model $\hat{H}_B(k) = h_x(k) \hat{\sigma}_x + h_y(k) \hat{\sigma}_y + m \hat{\sigma}_z$ with $h_x(k) = 1 + \delta + (1 - \delta) \cos k$, $h_y(k) = (1 - \delta) \sin k$, where $\hat{\sigma}_{x,y,z}$ are the Pauli operators. At $m = 0$, the Hamiltonian reduces to the SSH model and can be characterized by the topological invariant given by the winding number

ν [83, 101–103]. The trivial dimerization limit $\delta = 1$ corresponds to the $\nu = 0$, while $\delta = -1$ corresponds to the topological phase, $\nu = 1$, supporting the two zero-energy edge states in open boundary condition geometry.

The experimental platform for the considered quantum system has been realized in spinful fermions using ^{171}Yb atoms [88], and more recently with potassium ^{40}K atoms [91]. The characteristic temperature related to the recoil energy in this case is $T_0 \sim 200$ nK.

Results— The Rice-Mele Hamiltonian, Eq. (3), can serve as a quasi-optimal local quantum thermometer with open boundary conditions for specific fillings $f = N/L$, with $N = L/2 - 1$ or $N = L/2$ particles, where the optimal energy gap can be tuned by the dimerization parameter δ , and the staggered potential amplitude m .

We start with an analysis of the energy level spectrum for the SSH model, with vanishing staggered potential amplitude $m = 0$. We consider a lattice with $L = 14, 16$ sites and open boundary conditions with $N = L/2 - 1$, and $N = L/2$ particles. With the full many-body exact diagonalization, we calculate energy level spectra of the Hamiltonian Eq. (3) for each tuple $\{L, N, \delta\}$, $\delta \in [-1, 1]$, presented in Fig. 2. Panels (a)-(c) correspond to $N = L/2 - 1$ particles. The optimal energy level structure is realized at the topological dimerization limit, $\delta = -1$, where the system has a single ground state and degenerated first excited state with $2N$ -fold degeneracy. At $\delta = 1$, energy levels contain quasi-degeneracy of the ground state, resembling the energy level structure known from critical thermometry Ref. [53]. Panels (b)-(d) correspond to $N = L/2$ particles, where the optimal local quantum thermometer energy level structure is realized at trivial dimerization limit $\delta = 1$ with N^2 -fold degeneracy of the first excited state. For the $N = L/2 - 1$ particles and $\delta < 0$ the system realizes the quasi-optimal thermometer with quasi-degeneracy in the first excited state. In contrast, for $\delta \geq 0$, the system enters a single quasi-degenerated manifold regime, which is also characterized by high sensitivity to temperature changes [45, 53]. In the following, we study the thermometer’s sensitivity to temperature changes quantified by the quantum Fisher information.

Quantum Fisher information for the SSH model— We assume the thermometer is already in the thermal state at temperature T , given by $\hat{\rho}_T^B$. We focus on the quantum Fisher information, \mathcal{F}_T , Eq. (1) to characterize the system’s sensitivity to temperature changes.

Fig. 3(a)-(b) represents the quantum Fisher information \mathcal{F}_T , as a function of temperature T for fixed δ (thin solid lines) for $N = L/2 - 1$ and $N = L/2$ particles respectively. The thick, solid blue line represents the maximal \mathcal{F}_T envelope for different values of δ . The thermometer’s QFI is close to the QFI of the optimal local quantum thermometer $\bar{\mathcal{F}}_T$, Eq. (2). In panels (a)-(b), the dash-dotted black line corresponds to QFI of the optimal local quantum thermometer with $2N$ -fold degeneracy, while the dashed black line to $(D - 1)$ -fold degeneracy, corresponding to the situation where all energy

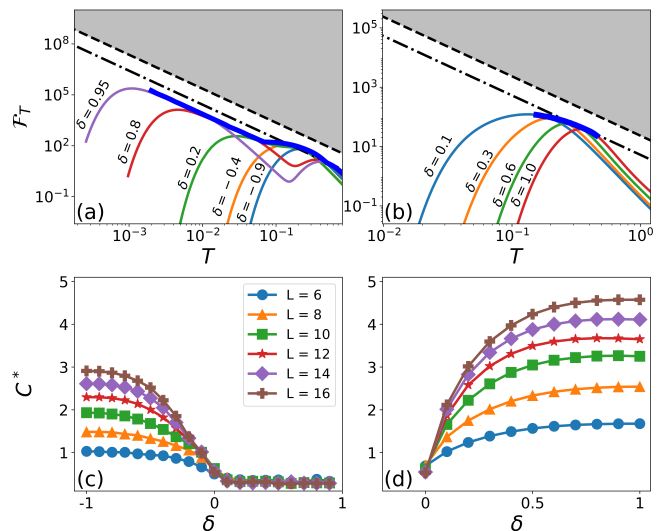


FIG. 3. Top row: (log-log scale) The sensitivity of the SSH quantum thermometer to the temperature changes in terms of QFI for $L = 16$ sites. Panel (a) corresponds to $N = L/2 - 1$, while panel (b) to $N = L/2$ particles. Solid thin lines represent \mathcal{F}_T as a function of temperature T , for different values of the dimerization parameter δ . The thick, solid blue line represents an envelope of the maximal QFI. The dashed line represents the QFI bound for an optimal local quantum thermometer with degeneracy corresponding to the total Hilbert space dimension D , while the dash-dotted line represents the QFI bound for the optimal quantum thermometer corresponding to the $2N$ -fold quasi-degenerated first excited state. For $T \gtrsim 10^{-1}$ in panel (a), the higher energy levels start to contribute, and hence the envelope may surpass the fundamental bound (dash-dotted line) where only the first manifold is considered. Bottom row: the maximal specific heat capacity C^* (see main text) as a function of δ , with increasing system size L for (c) $N = L/2 - 1$ and (d) $N = L/2$ fermions.

levels form the optimal energy level structure. The QFI has a peaked structure with the peak at an optimal temperature $T^* = \arg \max_T \mathcal{F}_T$, at which the measurement accuracy is maximized. The position of the peak of QFI can be controlled by tuning the dimerization strength δ .

The potential of a given thermometer for thermometry tasks is encoded into a more physically relevant quantity which is its specific heat capacity [39, 72]. Here, we consider the maximal specific heat capacity C^* of the thermometer, which is defined as $C^* = \mathcal{F}_{T^*} T^{*2}$, where T^* is the optimal temperature for a given set of model parameters $\{L, N, \delta\}$. Fig. 3 (c)-(d) present C^* vs δ for fixed system size L with $N = L/2 - 1$ and $N = L/2$ particles respectively. Specific heat capacity shows the advantage of the topological dimerization regime ($\delta < 0$) over the trivial one ($\delta > 0$) in scaling with the system size.

Quantum Fisher information for the Rice-Mele model— The crucial aspect of the practical utilization of this system as a local quantum thermometer is its energy gap tunability. Here, we show that controlling the

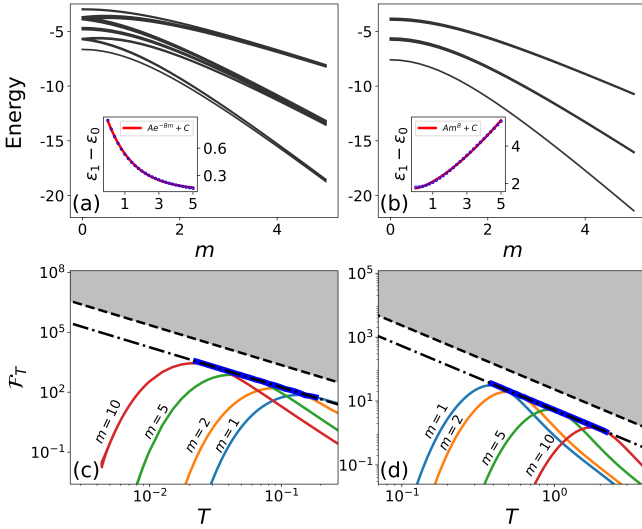


FIG. 4. Top row: Energy level spectrum as a function of the staggered potential amplitude m for $L = 16$ with (a) $N = L/2 - 1$ and $\delta = -1$, and (b) $N = L/2$ with $\delta = 1$. Insets present the fit (solid red lines) to the energy gap (blue dots) between the ground state and the first excited energy manifold. Bottom row: (log-log scale) quantum Fisher information \mathcal{F}_T for various m (thin solid lines) and the corresponding maximal quantum Fisher information envelope (thick solid blue line). The dashed line represents the QFI bound for an optimal local quantum thermometer [39] with degeneracy in the excited state manifold corresponding to the Hilbert space dimension D , and the dash-dotted line denotes the QFI bound for optimal local quantum thermometer with the quasi-degeneracy corresponding to the first excited state manifold in the energy spectrum (panels (a)-(b)).

staggered potential amplitude m allows adjusting the system's sensitivity over a few orders of magnitude of temperature changes. In Fig. 4(a)-(b), we present an energy level spectrum as a function of the staggered potential amplitude m with $N = L/2 - 1$ and $N = L/2$ particles, respectively, for $L = 16$ sites. For $N = L/2 - 1$ the first excited state has N -fold degeneracy, and N^2 -fold degeneracy for $N = L/2$ particles. The energy gap between the ground state and the first excited state manifold decreases exponentially [104] for $N = L/2 - 1$, while for $N = L/2$, the gap increases [105] with increasing staggered potential m .

In Fig. 4(c)-(d), we present the quantum Fisher information \mathcal{F}_T of the Hamiltonian with fixed dimerization parameter $\delta = -1$ (panel (c), $N = L/2 - 1$) and $\delta = 1$ (panel (d), $N = L/2$) for different values of the staggered potential amplitude m (thin solid lines). The control over the staggered potential m allows tuning the thermometer to the optimal temperature over three orders of magnitude by changing the position of the peak of quantum Fisher information \mathcal{F}_T .

Measurement protocol— Bounding the sensitivity given by the QFI requires preparing a measurement operator constructed from the eigenstates of the thermome-

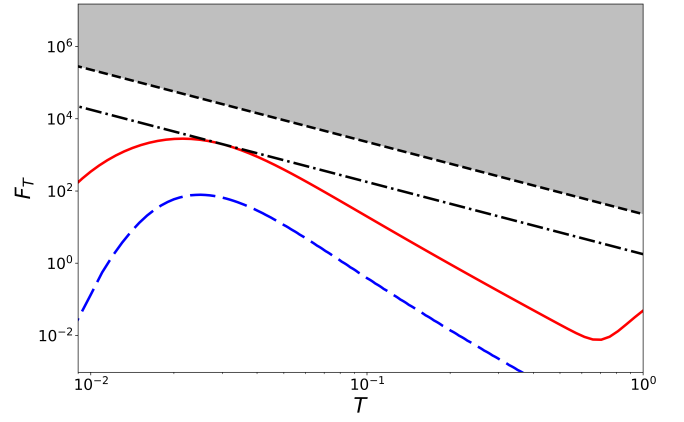


FIG. 5. Classical and quantum Fisher information for $N = L/2 - 1$, $L = 16$ lattice sites, topological dimerization limit $\delta = -1$, and staggered potential $m = 10$. The dashed blue lines present classical Fisher information, F_T , obtained from lattice site occupation measurements, while the red solid line represents the quantum Fisher information, \mathcal{F}_T , of the system. The dashed and dash-dotted lines denote the same as in Fig. 4.

ter Hamiltonian \hat{H}_B , which is challenging from the experimental point of view. To infer the sensitivity of the thermal state $\hat{\rho}_T^B$ of the thermometer to temperature changes from the measurements easily accessible in the experiment, we focus on the classical Fisher information $F_T = \sum_i \frac{1}{p_i(T)} \left(\frac{dp_i(T)}{dT} \right)^2$, where $p_i(T)$ are the probabilities of measurement outcomes. Here, as a measurement protocol, we consider the normalized lattice site occupation $p_i(T) = \text{Tr}[\hat{n}_i \hat{\rho}_T^B] / N$.

In Fig. 5, we show the classical Fisher information F_T for $L = 16$ sites, with $N = L/2 - 1$ at topological dimerization limit $\delta = -1$ with staggered potential amplitude $m = 10$. At the optimal temperature T^* , the quantum Fisher information \mathcal{F}_{T^*} has the same value as the quantum Fisher information $\bar{\mathcal{F}}_{T^*}$ for an idealized optimal local quantum thermometer with N -fold degeneracy of the excited state. The classical Fisher information at the optimal temperature is $F_{T^*} \simeq 10^2$, indicating the system's usefulness as a quantum thermometer.

Discussion and conclusions— We showed that the spinless fermions in a one-dimensional optical lattice described by the Rice-Mele model in open boundary conditions geometry can serve as an optimal local quantum thermometer operating in the sub-nK regime. Based on the parameter estimation theory, we analyzed the thermal sensitivity of the considered system in terms of quantum Fisher information. We showed that the staggered field amplitude can control the quantum thermometer's energy gap to match the estimated temperature, allowing us to maximize the sensitivity of the thermometer for a range of temperature values. Finally, we showed that the classical Fisher information obtained from more realistic and experimentally feasible lattice occupation measure-

ments is close to the quantum Fisher information limit.

The primary open question for utilizing the proposed quantum thermometer is about thermalization dynamics after coupling to another quantum system. Such a coupling can occur via contact interactions with another system of quantum particles confined in a lattice or via induced long-range Rydberg-dressed interactions leading to unconstrained energy transfer between the quantum thermometer [106, 107] and the quantum gas in a harmonic trap [108].

Acknowledgements— We thank Grzegorz Rajchel-Mieldzioć and Arkadiusz Kosior for carefully reading the manuscript. A.K.S. acknowledges support from the European Union’s Horizon 2020 Research and Innovation Programme under the Marie Skłodowska-Curie Grant Agreement No. 847517. M.P. acknowledges the support of the Polish National Agency for Academic Exchange, the Bekker programme no: PPN/BEK/2020/1/00317. ICFO group acknowledges support from: ERC AdG NO-QIA; MCIN/AEI (PGC2018-0910.13039/501100011033, CEX2019-000910-S/10.13039/501100011033, Plan National FIDEUA PID2019-106901GB-I00, Plan National STAMEENA PID2022-139099NB-I00 project funded by MCIN/AEI/10.13039/501100011033 and by the “European Union NextGenerationEU/PRTR” (PRTR-C17.I1), FPI); QUANTERA MAQS PCI2019-111828-2); QUANTERA DYNAMITE PCI2022-132919 (QuantERA II Programme co-funded by European Union’s

Horizon 2020 program under Grant Agreement No 101017733), Ministry of Economic Affairs and Digital Transformation of the Spanish Government through the QUANTUM ENIA project call – Quantum Spain project, and by the European Union through the Recovery, Transformation, and Resilience Plan – NextGenerationEU within the framework of the Digital Spain 2026 Agenda; Fundació Cellex; Fundació Mir-Puig; Generalitat de Catalunya (European Social Fund FEDER and CERCA program, AGAUR Grant No. 2021 SGR 01452, QuantumCAT U16-011424, co-funded by ERDF Operational Program of Catalonia 2014-2020); Barcelona Supercomputing Center MareNostrum (FI-2023-1-0013); EU Quantum Flagship (PASQuanS2.1, 101113690); EU Horizon 2020 FET-OPEN OPTologic (Grant No 899794); EU Horizon Europe Program (Grant Agreement 101080086 — NeQST), ICFO Internal “QuantumGaudi” project; European Union’s Horizon 2020 program under the Marie Skłodowska-Curie grant agreement No 847648; “La Caixa” Junior Leaders fellowships, La Caixa” Foundation (ID 100010434): CF/BQ/PR23/11980043. Views and opinions expressed are, however, those of the author(s) only and do not necessarily reflect those of the European Union, European Commission, European Climate, Infrastructure and Environment Executive Agency (CINEA), or any other granting authority. Neither the European Union nor any granting authority can be held responsible for them.

-
- [1] H. T. Quan, Y. Liu, C. P. Sun, and F. Nori, *Physical Review E* **76**, 031105 (2007).
 - [2] R. Kosloff and A. Levy, *Annual Review of Physical Chemistry* **65**, 365 (2014).
 - [3] M. Campisi, J. Pekola, and R. Fazio, *New Journal of Physics* **17**, 035012 (2015).
 - [4] J. P. S. Peterson, T. B. Batalhão, M. Herrera, A. M. Souza, R. S. Sarthour, I. S. Oliveira, and R. M. Serra, *Physical Review Letters* **123**, 240601 (2019).
 - [5] N. M. Myers, O. Abah, and S. Deffner, *AVS Quantum Science* **4**, 027101 (2022).
 - [6] J. Gemmer, M. Michel, and G. Mahler, *Quantum thermodynamics: Emergence of thermodynamic behavior within composite quantum systems*, Vol. 784 (Springer, 2009).
 - [7] S. Vinjanampathy and J. Anders, *Contemporary Physics* **57**, 545 (2016).
 - [8] J. Goold, M. Huber, A. Riera, L. del Rio, and P. Skrzypczyk, *Journal of Physics A: Mathematical and Theoretical* **49**, 143001 (2016).
 - [9] F. Binder, L. A. Correa, C. Gogolin, J. Anders, and G. Adesso, *Fundamental Theories of Physics* **195**, 1 (2018).
 - [10] S. Deffner and S. Campbell, *Quantum Thermodynamics*, 2053-2571 (Morgan & Claypool Publishers, 2019).
 - [11] S. Bhattacharjee and A. Dutta, *The European Physical Journal B* **94**, 1 (2021).
 - [12] S. Julià-Farré, T. Salamon, A. Riera, M. N. Bera, and M. Lewenstein, *Physical Review Research* **2**, 023113 (2020).
 - [13] S. Mondal and S. Bhattacharjee, *Physical Review E* **105**, 044125 (2022).
 - [14] S. Ghosh, T. Chanda, and A. Sen(De), *Physical Review A* **101**, 032115 (2020).
 - [15] S. Ghosh, T. Chanda, S. Mal, and A. Sen(De), *Physical Review A* **104**, 032207 (2021).
 - [16] D. T. Hoang, F. Metz, A. Thomasen, T. D. Anh-Tai, T. Busch, and T. Fogarty, Variational quantum algorithm for ergotropy estimation in quantum many-body batteries (2023), [arXiv:2308.03334 \[quant-ph\]](https://arxiv.org/abs/2308.03334).
 - [17] M. Boubakour, T. Fogarty, and T. Busch, *Physical Review Research* **5**, 013088 (2023).
 - [18] J. Koch, K. Menon, E. Cuestas, S. Barbosa, E. Lutz, T. Fogarty, T. Busch, and A. Widera, *Nature* **621**, 723 (2023).
 - [19] A. E. Leanhardt, T. A. Pasquini, M. Saba, A. Schirrotzek, Y. Shin, D. Kielpinski, D. E. Pritchard, and W. Ketterle, *Science* **301**, 1513 (2003).
 - [20] P. Medley, D. M. Weld, H. Miyake, D. E. Pritchard, and W. Ketterle, *Physical Review Letters* **106**, 195301 (2011).
 - [21] M. Horodecki and J. Oppenheim, *Nature Communications* **4**, 2059 (2013).
 - [22] L. D. Carlos and F. Palacio, *Thermometry at the nanoscale: techniques and selected applications* (Royal Society of Chemistry, 2015).
 - [23] K. V. Hovhannisyanyan and L. A. Correa, *Physical Review B* **98**, 045101 (2018).

- [24] P. Lipka-Bartosik, M. Perarnau-Llobet, and N. Brunner, *Physical Review Letters* **130**, 040401 (2023).
- [25] S. Bhattacharjee, U. Bhattacharya, and A. Dutta, *Physical Review B* **98**, 104302 (2018).
- [26] S. L. Braunstein and C. M. Caves, *Physical Review Letters* **72**, 3439 (1994).
- [27] H. Cramér, *Mathematical Methods of Statistics (PMS-9), Volume 9* (Princeton University Press, Princeton, 1946).
- [28] C. W. Helstrom, *Journal of Statistical Physics* **1**, 231 (1969).
- [29] V. Giovannetti, S. Lloyd, and L. Maccone, *Nature Photonics* **5**, 222 (2011).
- [30] L. Pezzè, A. Smerzi, M. K. Oberthaler, R. Schmied, and P. Treutlein, *Reviews of Modern Physics* **90** (2018).
- [31] A. K. Pati, C. Mukhopadhyay, S. Chakraborty, and S. Ghosh, *Physical Review A* **102**, 012204 (2020).
- [32] R. Demkowicz-Dobrzański, W. Górecki, and M. Guţă, *Journal of Physics A: Mathematical and Theoretical* **53**, 363001 (2020).
- [33] G. Müller-Rigat, A. K. Srivastava, S. Kurdziałek, G. Rajchel-Mieldzioc, M. Lewenstein, and I. Frérot, *Quantum* **7**, 1152 (2023).
- [34] I. Frérot, M. Fadel, and M. Lewenstein, *Reports on Progress in Physics* **86**, 114001 (2023).
- [35] S. Campbell, M. Mehboudi, G. D. Chiara, and M. Paternostro, *New Journal of Physics* **19**, 103003 (2017).
- [36] W.-K. Mok, K. Bharti, L.-C. Kwek, and A. Bayat, *Communications Physics* **4**, 62 (2021).
- [37] J. Rubio, J. Anders, and L. A. Correa, *Physical Review Letters* **127**, 190402 (2021).
- [38] J. Glatthard, J. Rubio, R. Sawant, T. Hewitt, G. Barontini, and L. A. Correa, *PRX Quantum* **3**, 040330 (2022).
- [39] L. A. Correa, M. Mehboudi, G. Adesso, and A. Sanpera, *Physical Review Letters* **114**, 220405 (2015).
- [40] A. De Pasquale, D. Rossini, R. Fazio, and V. Giovannetti, *Nature Communications* **7**, 12782 (2016).
- [41] A. De Pasquale and T. M. Stace, in *Thermodynamics in the Quantum Regime: Fundamental Aspects and New Directions* (Springer International Publishing, Cham, 2018) pp. 503–527.
- [42] M. Mehboudi, A. Sanpera, and L. A. Correa, *Journal of Physics A: Mathematical and Theoretical* **52**, 303001 (2019).
- [43] J. Boeyens, S. Seah, and S. Nimmrichter, *Physical Review A* **104**, 052214 (2021).
- [44] M. Mehboudi, M. R. Jørgensen, S. Seah, J. B. Brask, J. Kołodyński, and M. Perarnau-Llobet, *Physical Review Letters* **128**, 130502 (2022).
- [45] M. Płodzień, R. Demkowicz-Dobrzański, and T. Sowiński, *Physical Review A* **97**, 063619 (2018).
- [46] M. Płodzień, D. Wiater, A. Chrostowski, and T. Sowiński, Numerically exact approach to few-body problems far from a perturbative regime (2018), [arXiv:1803.08387 \[cond-mat.quant-gas\]](https://arxiv.org/abs/1803.08387).
- [47] M. Zgirski, M. Foltyn, A. Savin, K. Norowski, M. Meschke, and J. Pekola, *Physical Review Applied* **10**, 044068 (2018).
- [48] F. Brange, P. Samuelsson, B. Karimi, and J. P. Pekola, *Physical Review B* **98**, 205414 (2018).
- [49] D. Brody and N. Rivier, *Physical Review E* **51**, 1006 (1995).
- [50] P. Zanardi, P. Giorda, and M. Cozzini, *Physical Review Letters* **99**, 100603 (2007).
- [51] C. Invernizzi, M. Korbman, L. Campos Venuti, and M. G. A. Paris, *Physical Review A* **78**, 042106 (2008).
- [52] M. Mehboudi, L. A. Correa, and A. Sanpera, *Physical Review A* **94**, 042121 (2016).
- [53] E. Aybar, A. Niezgodna, S. S. Mirkhalaf, M. W. Mitchell, D. Benedicto Orenes, and E. Witkowska, *Quantum* **6**, 808 (2022).
- [54] G. W. Walker, V. C. Sundar, C. M. Rudzinski, A. W. Wun, M. G. Bawendi, and D. G. Nocera, *Applied Physics Letters* **83**, 3555 (2003).
- [55] F. Haupt, A. Imamoglu, and M. Kroner, *Physical Review Applied* **2**, 024001 (2014).
- [56] F. Seilmeier, M. Hauck, E. Schubert, G. J. Schinner, S. E. Beavan, and A. Högele, *Physical Review Applied* **2**, 024002 (2014).
- [57] E. Chekhovich, A. Ulhaq, E. Zallo, F. Ding, O. Schmidt, and M. Skolnick, *Nature Materials* **16**, 982 (2017).
- [58] M. Fujiwara and Y. Shikano, *Nanotechnology* **32**, 482002 (2021).
- [59] S. Razavian, C. Benedetti, M. Bina, Y. Akbari-Kourbolagh, and M. G. A. Paris, *The European Physical Journal Plus* **134**, 284 (2019).
- [60] C. Sabín, A. White, L. Hacker Muller, and I. Fuentes, *Scientific Reports* **4**, 1 (2014).
- [61] L. A. Correa, M. Perarnau-Llobet, K. V. Hovhannisyán, S. Hernández-Santana, M. Mehboudi, and A. Sanpera, *Physical Review A* **96** (2017).
- [62] M. Mehboudi, A. Lampo, C. Charalambous, L. A. Correa, M. Á. García-March, and M. Lewenstein, *Physical Review Letters* **122**, 030403 (2019).
- [63] M. M. Khan, M. Mehboudi, H. Terças, M. Lewenstein, and M. A. Garcia-March, *Physical Review Research* **4**, 023191 (2022).
- [64] J. Glatthard and L. A. Correa, *Quantum* **6**, 705 (2022).
- [65] R. S. Lous, I. Fritsche, M. Jag, B. Huang, and R. Grimm, *Physical Review A* **95**, 053627 (2017).
- [66] M. T. Mitchison, T. Fogarty, G. Guarnieri, S. Campbell, T. Busch, and J. Goold, *Physical Review Letters* **125**, 080402 (2020).
- [67] M. T. Mitchison, T. Fogarty, G. Guarnieri, S. Campbell, T. Busch, and J. Goold, *Physical Review Letters* **125**, 080402 (2020).
- [68] L. Oghittu and A. Negretti, *Physical Review Research* **4** (2022).
- [69] R. R. Rodríguez, M. Mehboudi, M. Horodecki, and M. Perarnau-Llobet, Strongly coupled fermionic probe for nonequilibrium thermometry (2023), [arXiv:2310.14655 \[quant-ph\]](https://arxiv.org/abs/2310.14655).
- [70] S. Robles and J. Rodríguez-Laguna, *Journal of Statistical Mechanics: Theory and Experiment* **2017**, 033105 (2017).
- [71] E. Martín-Martínez, A. Dragan, R. B. Mann, and I. Fuentes, *New Journal of Physics* **15**, 053036 (2013).
- [72] P. Abiuso, P. A. Erdman, M. Ronen, F. Noé, G. Haack, and M. Perarnau-Llobet, Optimal thermometers with spin networks (2023), [arXiv:2211.01934 \[quant-ph\]](https://arxiv.org/abs/2211.01934).
- [73] M. Brenes and D. Segal, *Physical Review A* **108**, 032220 (2023).
- [74] A. Dawid, J. Arnold, B. Requena, A. Gresch, M. Płodzień, K. Donatella, K. A. Nicoli, P. Stornati, R. Koch, M. Büttner, R. Okuła, G. Muñoz-Gil, R. A. Vargas-Hernández, A. Cervera-Lierta, J. Carrasquilla, V. Dunjko, M. Gabrié, P. Huembeli, E. van

- Nieuwenburg, F. Vicentini, L. Wang, S. J. Wetzel, G. Carleo, E. Greplová, R. Krems, F. Marquardt, M. Tomza, M. Lewenstein, and A. Dauphin, Modern applications of machine learning in quantum sciences (2022), [arXiv:2204.04198 \[quant-ph\]](#).
- [75] F. S. Luiz, A. d. O. Junior, F. F. Fanchini, and G. T. Landi, *Physical Review A* **105**, 022413 (2022).
- [76] R. Salvia, M. Mehboudi, and M. Perarnau-Llobet, *Physical Review Letters* **130**, 240803 (2023).
- [77] M. J. Rice and E. J. Mele, *Physical Review Letters* **49**, 1455 (1982).
- [78] W. P. Su, J. R. Schrieffer, and A. J. Heeger, *Physical Review Letters* **42**, 1698 (1979).
- [79] A. J. Heeger, S. Kivelson, J. R. Schrieffer, and W. P. Su, *Reviews of Modern Physics* **60**, 781 (1988).
- [80] X.-L. Qi and S.-C. Zhang, *Reviews of Modern Physics* **83**, 1057 (2011).
- [81] M. Z. Hasan and C. L. Kane, *Reviews of Modern Physics* **82**, 3045 (2010).
- [82] S. Ryu, A. P. Schnyder, A. Furusaki, and A. W. W. Ludwig, *New Journal of Physics* **12**, 065010 (2010).
- [83] J. K. Asbóth, L. Oroszlány, and A. Pályi, *A Short Course on Topological Insulators* (Springer International Publishing, 2016).
- [84] J. Argüello-Luengo, U. Bhattacharya, A. Celi, R. W. Chhajlany, T. Grass, M. Płodzień, D. Rakshit, T. Salamon, P. Stornati, L. Tarruell, and M. Lewenstein, Synthetic dimensions for topological and quantum phases: Perspective (2023), [arXiv:2310.19549 \[quant-ph\]](#).
- [85] M. Atala, M. Aidelsburger, J. T. Barreiro, D. Abanin, T. Kitagawa, E. Demler, and I. Bloch, *Nature Physics* **9**, 795 (2013).
- [86] A. Hayward, C. Schweizer, M. Lohse, M. Aidelsburger, and F. Heidrich-Meisner, *Physical Review B* **98**, 245148 (2018).
- [87] M. Lohse, C. Schweizer, O. Zilberberg, M. Aidelsburger, and I. Bloch, *Nature Physics* **12**, 350 (2015).
- [88] S. Nakajima, T. Tomita, S. Taie, T. Ichinose, H. Ozawa, L. Wang, M. Troyer, and Y. Takahashi, *Nature Physics* **12**, 296 (2016).
- [89] G. H. Reid, M. Lu, A. R. Fritsch, A. M. Piñeiro, and I. B. Spielman, *Physical Review Letters* **129**, 123202 (2022).
- [90] N. R. Cooper, J. Dalibard, and I. B. Spielman, *Reviews of Modern Physics* **91**, 015005 (2019).
- [91] A.-S. Walter, Z. Zhu, M. Gächter, J. Minguzzi, S. Roschinski, K. Sandholzer, K. Viebahn, and T. Esslinger, *Nature Physics* **19**, 1471 (2023).
- [92] X. Li, Y. Meng, X. Wu, S. Yan, Y. Huang, S. Wang, and W. Wen, *Applied Physics Letters* **113**, 203501 (2018).
- [93] D. J. Rizzo, G. Veber, T. Cao, C. Bronner, T. Chen, F. Zhao, H. Rodriguez, S. G. Louie, M. F. Crommie, and F. R. Fischer, *Nature* **560**, 204 (2018).
- [94] L. Li, Z. Xu, and S. Chen, *Physical Review B* **89**, 085111 (2014).
- [95] K. Giergiel, A. Dauphin, M. Lewenstein, J. Zakrzewski, and K. Sacha, *New Journal of Physics* **21**, 052003 (2019).
- [96] S. de Léséleuc, V. Lienhard, P. Scholl, D. Barredo, S. Weber, N. Lang, H. P. Büchler, T. Lahaye, and A. Browaeys, *Science* **365**, 775 (2019).
- [97] S. Weber, S. de Léséleuc, V. Lienhard, D. Barredo, T. Lahaye, A. Browaeys, and H. P. Büchler, *Quantum Science and Technology* **3**, 044001 (2018).
- [98] V. Lienhard, S. de Léséleuc, P. Scholl, D. Barredo, T. Lahaye, and A. Browaeys, in *Quantum Information and Measurement (QIM) V: Quantum Technologies* (Optica Publishing Group, 2019) p. F4B.2.
- [99] L. Jing, J. Xiao-Xing, Z. Wei, and W. Xiao-Guang, *Communications in Theoretical Physics* **61**, 45 (2014).
- [100] In the limit of large degeneracy of the excited state, i.e. $D \rightarrow \infty$, one can approximate $x \simeq \ln D$, $2\sqrt{f(D)} \simeq \ln D$, maximal QFI reads $\overline{\mathcal{F}}_T = (\ln D/2T)^2$, and the relative temperature estimation accuracy is bounded from below by $\Delta T/T \geq 2/\sqrt{N} \ln D$.
- [101] R. Resta, *Physical Review Letters* **80**, 1800 (1998).
- [102] R. Resta, *Reviews of Modern Physics* **66**, 899 (1994).
- [103] S. Sen and K. S. Gupta, *Many-Body Physics, Topology and Geometry* (World Scientific, 2015).
- [104] $y = Ae^{-Bm} + C$;
 $\{A, B, C\} = \{0.76418, 0.64130, 0.13517\}$.
- [105] $y = Am^B + C$;
 $\{A, B, C\} = \{0.35598, 1.44097, 1.74417\}$.
- [106] T. Macrì and T. Pohl, *Physical Review A* **89**, 011402 (2014).
- [107] D. Malz and J. I. Cirac, *PRX Quantum* **4**, 020301 (2023).
- [108] M. Płodzień, G. Lochead, J. de Hond, N. J. van Druuten, and S. Kokkelmans, *Physical Review A* **95**, 043606 (2017).